Resting-state brain networks in functional MRI

Pierre Bellec[1], Arnaud Messé[2,3], David Coynel[2,3], Vincent Perlbarg[2,3], Habib Benali[1,2,3], Guillaume Marrelec[1,2,3]

[1] UNF, Geriatric Institute, University of Montreal, Montreal, Canada H3W 1W5

[2] U678, Inserm, Paris, F-75013 France

[3] Faculté de médecine Pitié-Salpêtrière, UPMC Univ Paris 06, Paris, F-75013 France

Contraintes. 10 printed pages, 3000 characters per page, 5 figures (with the possibility to put additional figures on-line), up to 50 references.

1 Introduction

Blood oxygen level dependent (BOLD) functional magnetic resonance imaging (fMRI) has been extensively used to study how task performance modulates brain activity. Such an approach emphasizes the principle of functional segregation, in that different brain areas are characterized by their involvement in specific cognitive processes. However, this type of analysis essentially ignores that the brain maintains a constant level of spontaneous activity, i.e., activity that is not a direct consequence of environmental stimulations. Investigating these spontaneous brain fluctuations is a challenge precisely because they cannot be controlled by an experimental design. The first successful study of brain spontaneous fluctuations in BOLD fMRI was performed by Biswal and colleagues, who computed the correlation between the time course of a seed region and all brain voxels in the absence of any experimental task (Biswal et al., 1995). Such resting-state functional connectivity maps, which identified distributed sets of brain regions whose spontaneous activity exhibited a large degree of temporal coherence, are currently known as resting-state networks (RSNs). By contrast with task-oriented studies, investigation of RSNs relies on the principle of functional integration: brain regions are characterized by the set of regions with which their signal is highly synchronized.

While the exact mechanisms at the origin of spontaneous fluctuations are still not fully elucidated, it is now firmly established that RSNs are mainly the consequence of neural activity. Approaches combining multiple neuroimaging modalities have contributed to better understand their neuronal and anatomical basis. Much progress has also been done regarding methods, with the emergence of fully exploratory multivariate techniques. Beyond the mapping of RSNs, some recent approaches use a graph representation which gives a better insight into the structure of information flow within RSNs.

Investigation of RSNs in BOLD fMRI is a recent yet quickly growing field that has already generated a wealth of applications. This chapter is a concise review of the most prominent results and challenges, as well as a discussion of existing and potential applications. References were carefully selected to point the interested readers to key works as well as some specialized reviews that cover the various topics presented here more thoroughly.

2 Mapping RSNs

In the present section, we summarize the main methods used to map the spatial distributions of RSNs and we also present a typology of the maps that have been reported so far in the literature.

2.1 Methods

Mapping RSNs consists of finding sets of voxels that exhibit coherent spontaneous BOLD fluctuations. In a seminal work on resting-state fMRI, Biswal et al. (1995) introduced functional connectivity maps, i.e., volumes representing the correlation between the time course of a seed region and that of every

voxel in the brain (see Figure 1). A variety of fully exploratory and multivariate algorithms have then been proposed to automatically identify RSNs without having to rely on the choice of a particular seed region, see Li et al. (2009) for a review. The most popular of these techniques is spatial independent component analysis (ICA) (see Figure 2). The significant ICA maps delineate groups of brain regions that seem interpretable in terms of brain networks. Such identification is performed at the level of a single subject; for group-level analyses, the methodology needs to be extended to identify group-level RSNs that would summarize the distribution of individual maps across many subjects. The first and still popular approach for group ICA essentially consists of concatenating subjects in time and run a standard ICA on the concatenated time series to derive group components. Many methodological challenges remain in this area, which is still under active development, see Calhoun et al. (2009) for an excellent review of recent approaches. In the perspective of clinical applications, perhaps the most important of these open challenges is to propose a framework that will be flexible enough to capture individual variability, while still allowing for a clear correspondence between group-level and individual-level RSNs.

2.2 Reliability of extracted maps

A key question is the degree of reliability of the extracted maps, which can be affected by two main factors. The first one is algorithmic: how does the choice of algorithm and parameters impact the maps? The second one is related to the particular sample of datasets that is selected for the study: how stable would be the maps if the study were to be replicated with a new, independent database? Altogether, the RSNs reported so far in the literature exhibit a fair level of agreement across studies (see Section 2.3), suggesting that RSN identification is overall reliable.

Regarding algorithmic reliability, Margulies et al. (2009) showed that even a small shift of the seed voxel could lead to dramatic instability of the connectivity pattern (see Figure 4). Similar results were reported using slightly different ROIs within the default mode network (see Section 2.3 for definition and description of that particular RSN) (Buckner et al., 2008; Cole et al., 2010). As to RSN extraction by spatial ICA, it was found that the algorithm used was rather robust to its initial conditions. Few studies have compared specific RSNs identified by different methods (e.g., connectivity maps and ICA). The existing results suggest a good level of agreement across methods, yet many of the alternatives to ICA have not yet been included in such investigation.

Regarding sampling reliability, an early work had concluded to a high degree of reproducibility of some specific RSNs identified using ICA both across subjects and across datasets acquired on the same subject. More systematic extensions of this study to test-retest databases found moderate to high reliability at the group level Van Dijk et al. (2010); Zuo et al. (2010). Tests-retest stability can be approximated from a single sample of the population using resampling techniques. The work of Damoiseaux et al. (2006) was notably the first to claim the consistency of group RSNs using this type of approach.

2.3 Typology of RSNs

The sensorimotor network was the first RSN studied with functional connectivity using a seed in the primary motor cortex (Biswal et al., 1995). A visual RSNs was identified with a seed around the calcarine fissure, and a limbic network with a seed in the amygdala. An auditory and a language RSNs were later extracted as well as a fronto-parietal network involved notably in working-memory tasks. The so called default-mode network (DMN) was also identified using a seed in the posterior cingulate cortex. Interestingly, this network was first defined as a set of regions consistently exhibiting larger BOLD activity during rest periods than during a broad range of task-oriented behaviors, and in addition has the highest level of metabolic activity in the brain. These networks could also be identified in a reliable manner through ICA (Damoiseaux et al., 2006) (see Figure 3 for a summary of findings at the group level). An interesting phenomenon which can occur in ICA is the splitting of a network in one or more subnetworks (e.g. the subdivision of the visual cortex into primary and extrastriate) when the number of extracted

networks is large (Smith et al., 2009). The anatomofunctional significance of such fine RSNs cartography largely remains to be investigated, even though it has been shown to be consistent with the organization of the monkey brain as well as the organization of white matter tracts in some specific areas such as the precuneus (Margulies et al., 2009) (see Figure 4). For a more detailed typology of the RSNs along with Talairach coordinates, see Perlbarg and Marrelec (2008). For reviews that are specific to the default-mode network, see Raichle and Snyder (2007) or Buckner et al. (2008).

3 Investigating information flow within RSNs

Graph representations are perfectly suited to characterize information flow within RSNs. Graphs are composed of two objects: vertices or nodes (regions) and edges (links or connections), both of which can be defined using various techniques. Once a RSN has been modeled in the form of a graph, tools from graph theory can be used to summarize its key properties.

3.1 Defining nodes

Graph nodes are the functional units that are being connected. It is generally not feasible to identify each voxel with a specific node, because it would lead to analyses that are computationally very challenging. More fundamentally, the fMRI time courses within individual voxels are also highly redundant and noisy. It is therefore common practice to select a very limited set of regions (e.g., from 3 to 20) based on prior knowledge; each region is then defined as a sphere centered around a stereotaxic coordinate. Alternatively, a full brain exploration can be performed by grouping voxels into brain regions that are then used as nodes. A common strategy is to rely on an atlas of brain regions manually segmented on the basis of anatomical landmarks in a stereotaxic space of reference. However, this atlas has a limited number of regions (116), potentially gathering voxels with heterogeneous signal. To circumvent this issue and investigate graph properties at a finer spatial scale, one can either generate a gray matter parcellation of arbitrary size or reduce the number of voxels by resampling the data to a coarser resolution. Using functional data, brain regions can be obtained at the individual level as sets of voxels with highly homogeneous time courses; group-level studies then require to establish a correspondence between individual brain regions across subjects. Finally, brain regions based on structural (i.e., white matter) connectivity rather than functional connectivity has also been advocated.

3.2 Quantifying links

Once nodes have been selected, the strength of the connection between two nodes is usually quantified by their so-called functional connectivity, i.e., the temporal correlation between the time courses of these regions. Many studies have used correlation as a way to characterize connections between regions. Other statistical measures of functional connectivity have been proposed to circumvent certain shortcomings of correlation, such as conditional and partial correlations. Measures have been used either in the temporal or the frequency domain.

When the number of regions remains limited, the strength of connection between regions can also be quantified by effective connectivity, which considers the influence that regions exert on each other. The notion of effective connectivity is strongly tied with that of causality. The two main frameworks to investigate it are structural equation modeling (SEM) and dynamical causal modeling (DCM). Both approaches are model-based and strongly rely (at least to some level) on the definition of a structural model in the form of a directed graph prior to the analysis. While causality appears to be naturally embedded in SEM and DCM in the form of arrow directions, exploratory investigation of causal relationships remains a challenge. Few methods have been proposed in fMRI, with the notable exception of the application of Granger causality. To our knowledge, only one study has investigated effective connectivity within RSNs

(James et al., 2009). For a review on measures of functional and effective connectivity, see Marrelec et al. (2006) or Rogers et al. (2007).

3.3 Characterizing graphs

When the number of regions N increases, the number of potential connections increases as $N(N-1)/2$ (45 for $N = 10$, 4950 for $N = 100$) and direct interpretation of the graph and its connections quickly becomes impossible. For this reason, measures have been proposed that compute a global summary of the graph features. In statistics, such measures were proposed based notably on mutual information. Also, using graph theory, one can study the characteristic path length L of a network and its clustering coefficient C. Small-world networks are a variety of graphs whose properties lie between the two extreme configurations (random and lattice), with small L (comparable to random networks) and high C (comparable to lattice networks) (see Figure 5). In fMRI, the brain architecture was found to exhibit small-world properties. Many others measures exist, such as alternative measures of efficiency, modularity, or motifs. For a review of graph theory and its application to brain networks, see Bullmore and Sporns (2009), or van den Heuvel and Hulshoff Pol (in press).

3.4 Reliability of graph-theoretic measures

While the test-retest reliability of graph representation of RSNs has not been investigated to the best of our knowledge, a few studies have investigated the algorithmic reliability which is influenced by two factors: how nodes are selected and what signal is assigned to each node. Using two atlases of 90 and 70 regions, Wang et al. (2009) showed that node definition has an influence on the quantitative measures of graph theory, but not on the qualitative nature of the graph. Hayasaka and Laurenti (2010) compared voxel-based and region-based (with 90 regions) graphs and showed that even qualitative features of the graph could differ. As to the signal assigned to a node, it is usually the spatial average of the time courses of all voxels within a neighborhood. As will be discussed in the next section, removal of structured physiological processes is an important step and can modify the whole pattern of functional connectivity and, consequently, all graph-theoretic measures (Chang and Glover, 2009).

4 Neurophysiological basis of RSNs

Since the early controversy regarding the neural origin of resting-state BOLD fluctuations, a number of key aspects of the neurophysiological basis of RSNs have been established, namely: (1) RSNs are not only consequences of physiological noise; (2) RSNs reflect, to some extent, the underlying structural connections; (3) RSNs can be related to the neural activity as measured with other imaging modalities; and (4) RSNs represent sets of brain regions that are involved in similar functions.

4.1 Physiological noise

BOLD signal only accounts for part of fMRI signal, which also contains artifacts from various origins. In particular, some physiological processes (e.g., cardiac, respiratory, or movement-related) induce spurious effects that contaminate the BOLD signal in the whole brain. Nonetheless, it has been shown that spatially structured physiological fluctuations and spontaneous activity as measured by low-frequency BOLD signal seem to be two distinct processes. Still, physiological noise reduction is increasingly acknowledged as a key step in connectivity analysis and is commonly applied in recent studies (Biswal et al., 2010). There is however not yet an agreement regarding the best methodological approach to perform this noise reduction. For discussions on physiological noises, see, e.g., Marrelec et al. (2006), Rogers et al. (2007), Auer (2008) or Perlbarg and Marrelec (2008).

4.2 RSNs and structural connectivity

A key question for a better understanding of RSNs is the relationship between these networks and the underlying structural connectivity. In monkey, the DMN was found to be composed of regions that are connected to one another (Buckner et al., 2008). Also, the cortical pattern of correlation with oculomotor regions was found to be consistent with the anatomical connectivity pattern obtained by retrograde tracer injection (Vincent et al., 2007). In human, studies comparing maps of RSN and structural connectivity from diffusion-weighted imaging (DWI) showed that nodes that are functionally connected can, but do not need to, be anatomically connected (Greicius et al., 2009; van den Heuvel et al., 2009). Still, there is converging evidence that brain regions defined on the basis of either local homogeneity of functional connectivity or local homogeneity of structural connectivity are largely consistent with each other (Tomassini et al., 2007; Margulies et al., 2009) (see Figure 4). To elucidate the intricate relationship between the patterns of white matter connections and the emergence of functionally connected RSNs, a number of recent studies have implemented complex neurocomputational models whose objective is to replicate the dynamics of neuronal assemblies in a completely controlled, digital environment. The relationship between RSNs and the underlying structural connectivity is further reviewed in Damoiseaux and Greicius (2009) and van den Heuvel and Hulshoff Pol (in press) from an experimental perspective, while Honey et al. (in press) concentrates on more theoretical aspects.

4.3 RSNs and neural activity

The spontaneous fluctuations of brain activity as measured in BOLD fMRI have been compared to more direct measures of neural activity. Scalp electroencephalography (EEG), in particular, is a well-established tool to study resting-state activity. Many studies have used simultaneous EEG-fMRI acquisitions to investigate the fMRI correlates of EEG activity. The existence of a complex relationship between both types of signal was evidenced, relationship that depends on the features extracted from the EEG signal, see Laufs (2008) for a review. In monkey, cortical electrophysiological measure of the neural activity also concluded to a significant relationship with the BOLD spontaneous fluctuations (Shmuel and Leopold, 2008).

4.4 RSNs and neural correlates of cognitive functions

RSNs have also been found to be specifically involved in certain tasks. The DMN has consistently been reported as exhibiting blocked and event-related task-induced deactivation in human (Gusnard and Raichle, 2001). In monkey, the cortical pattern of correlation with oculomotor regions was found to be consistent with the response pattern evoked during performance of a saccadic eye movement task (Vincent et al., 2007). In human, a meta-analysis of task-related studies showed that voxels that were consistently coactivated during specific tasks formed networks that strikingly matched RSNs (Smith et al., 2009).

5 Applications

A key advantage of resting-state fMRI is that the acquisition protocol is very simple and requires no particular ability from the subject, so that it can be performed even by patients with impaired functions. It is now routinely performed for cognitive purposes and is also getting increasingly used in clinical research.

5.1 Healthy brain

Resting-state connectivity has been used as a tool in many areas of basic neuroscience. We focused here on a number of results that have a direct implication for the design of resting-state protocols in relation

with the following questions: (1) Can RSNs be identified during task performance? (2) Can RSNs be identified at any stage of brain development and aging?

Modulation of RSNs by a task A number of studies have looked at the modulation of RSNs by experimental tasks. For example, the spatial extent of the DMN was found to remain stable during a simple visual task (Greicius et al., 2003). Other studies have shown some modulation of the connectivity within the DMN by a task, e.g. as a function of the working memory load (Esposito et al., 2006). This kind of approach was also applied to a variety of other RSNs and tasks. More recently, ICA was used to assess systematically the stability of all RSNs in an oddball task (Calhoun et al., 2008).

Brain maturation Most of the RSNs found in adult could also be successfully extracted using sICA on resting-state acquisitions of children (Fransson et al., 2007). Using graph-theoretical measures, a similar global organization was found in children and young adults; however, development was characterized by a simultaneous reduction of short-range connectivity and a strengthening of long-range connectivity, suggesting a process of greater functional segregation in children and greater functional integration in young-adults at the whole-brain level (Superkar et al., 2009).

Aging RSNs were also studied in healthy aging. Graph-theoretic measures of global and local efficiency were altered in healthy older people in frontal, temporal and limbic/paralimbic cortical areas, as well as in subcortical areas such as the pallidum and thalamus. By contrast, the same cortical areas were identified as hubs in younger and older subjects (Achard and Bullmore, 2007). This loss of efficiency was consistent with results obtained from ICA, which revealed alterations in the DMN. Decreased activity was found in this network in healthy older as compared to healthy young subjects (Damoiseaux et al., 2008; Koch et al., in press), with anterior regions activity being inversely proportional to the score of cognitive tests measuring executive functioning and processing speed.

5.2 RSNs and pathologies

RSNs have been investigated in the context of a broad range of pathologies, including Alzheimer's disease, mental disorders, multiple sclerosis, and non-communicative patients, to name a few, see Auer (2008), Guye et al. (in press) or van den Heuvel and Hulshoff Pol (in press) for a review, and Mesulam (2009) for a discussion. At least three types of benefits could be gained from these investigations. First, RSNs have been evidenced to be sensitive to the progression of certain diseases and could therefore serve as biomarkers to predict their evolution. RSNs could also provide insight into the neural correlates of a disease and thus provide a better understanding of the underlying neurophysiological process. Finally, RSNs could be used to guide an intervention. These topics will respectively be illustrated with three pathologies: Alzheimer's disease (AD), non-communicative patients and brain tumors.

Alzheimer's disease A critical challenge in the treatment of AD is the identification of biomarkers for the early/prodromal diagnosis of the pathology. A seminal finding was that the regions belonging to the DMN exhibit a loss of connectivity in AD (Greicius et al., 2004). This promising preliminary result has not been yet followed by a full realization of the potential of RSNs as an early biomarker of AD. It was still recently showed that gray matter atrophy associated with AD follows the pattern of the DMN (see Figure 6). The small-world organization of brain activity, as characterized by the clustering coefficient, also seems to be altered by the pathology (Superkar et al., 2008). Increased correlations within prefrontal, parietal, and occipital lobes were also reported in AD patients, which could be interpreted as possible compensatory mechanisms (Wang et al., 2007).

Non-communicative patients While we are not aware of many studies using RSNs in the study of patients with traumatic brain injury, it can be expected that such studies will gain importance in the coming years. A longitudinal follow-up of patients scanned 3 and 6 month after TBI showed that, with recovery, graph-theoretical measures get closer to what is observed in healthy controls Nakamura et al. (2009). Interestingly, functional connectivity within the DMN in non-communicative patients was negatively correlated with the degree of clinical consciousness impairment Vanhaudenhuyse et al. (2010). This finding is consistent with the putative critical role of the DMN in self-oriented mental processes.

Brain tumors RSNs could be used not only to provide a diagnostic, but also to predict the response of a given patient to a particular treatment and plan the treatment accordingly. A few recent studies have provided a proof of concept in the context of preoperative mapping of the sensorimotor cortex, as part of the neurosurgical planning for brain tumor resection, e.g. (Kokkonen et al., 2009; Zhang et al., 2009; Shimony et al., 2009). Obviously, using RSNs for neurosurgical planning will require specific and thorough evaluation in terms of postoperative outcome. An important word of caution is that such a use entails strong assumptions regarding the relationships between the neurophysiological basis of the pathology and BOLD RSNs. Many non-neuronal factors can have an influence on the BOLD signal, a few of which being age, sedation, sleep, and disease. In this last category, the potential effects can be as varied as the pathologies themselves, ranging from a change in the vasculature and/or blood flow alteration (as in stroke), alteration of metabolism (as in glioma and other tumors), cortex properties (as in Alzheimer's disease). For these reasons, there is also a lot to gain in the understanding of RSNs themselves through their use in therapy.

References

Achard, S., Bullmore, E., 2007. Efficiency and cost of economical brain functional networks. PLoS Computational Biology 3, e17.

Auer, D. P., 2008. Spontaneous low-frequency blood oxygenation level-dependent fluctuations and functional connectivity analysis of the 'resting' brain. Magnetic Resonance Imaging 26, 1055–1064.

Biswal, B., Yetkin, F. Z., Haughton, V. M., Hyde, J. S., 1995. Functional connectivity in the motor cortex of resting human brain using echoplanar MRI. Magnetic Resonance in Medicine 34, 537–541.

Biswal, B. B., Mennes, M., Zuo, X. N., Gohel, S., Kelly, C., Smith, S. M., Beckmann, C. F., Adelstein, J. S., Buckner, R. L., Colcombe, S., Dogonowski, A. M., Ernst, M., Fair, D., Hampson, M., Hoptman, M. J., Hyde, J. S., Kiviniemi, V. J., Kötter, R., Li, S. J., Lin, C. P., Lowe, M. J., Mackay, C., Madden, D. J., Madsen, K. H., Margulies, D. S., Mayberg, H. S., McMahon, K., Monk, C. S., Mostofsky, S. H., Nagel, B. J., Pekar, J. J., Peltier, S. J., Petersen, S. E., Riedl, V., Rombouts, S. A., Rypma, B., Schlaggar, B. L., Schmidt, S., Seidler, R. D., Siegle, G. J., Sorg, C., Teng, G., Veijola, J., Villringer, A., Walter, M., Wang, L., Weng, X. C., Whitfield-Gabrieli, S., Williamson, P., Windischberger, C., Zang, Y. F., Zhang, H. Y., Castellanos, F. X., Milham, M. P., 2010. Toward discovery science of human brain function. Proceedings of the National Academy of Sciences of the U.S.A. 107, 4734–4739.

Buckner, R. L., Andrews-Hanna, J. R., Schacter, D. L., 2008. The brain's default network: anatomy, function, and relevance to disease. Annals of the New York Academy of Sciences 1124, 1–38.

Bullmore, E., Sporns, O., 2009. Complex brain networks: graph theoretical analysis of structural and functional systems. Nature Reviews Neuroscience 10, 186–198.

Calhoun, V. D., Kiehl, K. A., Pearlson, G. D., 2008. Modulation of temporally coherent brain networks estimated using ICA at rest and during cognitive tasks. Human Brain Mapping 29, 828–838.

Calhoun, V. D., Liu, J., Adali, T., 2009. A review of group ICA for fMRI data and ICA for joint inference of imaging, genetic, and ERP data. NeuroImage 45, S163–S172.

Chang, C., Glover, G. H., 2009. Effects of model-based physiological noise correction on default mode network anti-correlations and correlations. NeuroImage 47, 148–1459.

Cole, D. M., Smith, S. M., Beckmann, C. F., 2010. Advances and pitfalls in the analysis and interpretation of resting-state FMRI data. Frontiers in Systems Neuroscience 4, Article 8.

Damoiseaux, J. S., Beckmann, C. F., Sanz Arigita, E. J., Barkhof, F., Scheltens, P., Stam, C., Smith, S., Rombouts, S. A. R. B., 2008. Reduced resting-state brain activity in the "default network" in normal aging. Cerebral Cortex 18, 1856–1864.

Damoiseaux, J. S., Greicius, M. D., 2009. Greater than the sum of its parts: a review of studies combining structural connectivity and resting-state functional connectivity. Brain Structure and Function 213, 525–533.

Damoiseaux, J. S., Rombouts, S. A., Barkhof, F., Scheutens, P., Stam, C. J., .Smith, S. M., Beckmann, C. F., 2006. Consistent resting-state networks across healthy subjects. Proceedings of the National Academy of Sciences of the U.S.A. 103, 13848–13853.

Esposito, F., Bertolino, A., Scarabino, T., Latorre, V., Blasi, G., Popolizio, T., Tedeschi, G., Cirillo, S., Goebel, R., F.Di Salle, 2006. Independent component model of the default-mode brain function: Assessing the impact of active thinking. Brain Research Bulletin 70, 263–269.

Fransson, P., Skiöld, B., Horsch, S., Nordell, A., Blennow, M., Lagercrantz, H., Åden, U., 2007. Resting-state networks in the infant brain. Proceedings of the National Academy of Sciences of the U.S.A. 104, 15531–15536.

Greicius, M. D., Krasnow, B., Reiss, A. L., Menon, V., 2003. Functional connectivity in the resting brain: a network analysis of the default mode hypothesis. Proceedings of the National Academy of Sciences of the U.S.A. 100, 253–258.

Greicius, M. D., Srivastava, G., Reiss, A. L., Menon, V., 2004. Default-mode network activity distinguishes Alzheimer's desease from healthy aging: evidence from functional MRI. Proceedings of the National Academy of Sciences of the U.S.A. 101, 4637–4642.

Greicius, M. D., Supekar, K., Menon, V., Dougherty, R. F., 2009. Resting-state functional connectivity reflects structural connectivity in the default mode network. Cerebral Cortex 19, 72–78.

Gusnard, D. A., Raichle, M. E., 2001. Searching for a baseline: functional imaging and the resting human brain. Nature Reviews Neuroscience 2, 685–694.

Guye, M., Bettus, G., Bortolomei, F., Cozzone, P. J., in press. Graph theoretical analysis of structural and functional connecitvity MRI in normal and pathological brain networks. Magnetic Resonance Materials in Physics, Biology and Medicine .

Hayasaka, S., Laurenti, P. J., 2010. Comparison of characteristics between region-and voxel-based network analyses in resting-state fMRI data. NeuroImage 50, 498–508.

Honey, C. J., Thivierge, J.-P., Sporns, O., in press. Can structure predict function in the human brain? NeuroImage .

James, G. A., Kelley, M. E., Craddock, R. C., Holtzheimer, P. E., Dunlop, B. W., Nemeroff, C. B., Mayberg, H. S., Hu, X. P., 2009. Exploratory structural equation modeling of resting-state fMRI: Applicability of group models to individual subjects. NeuroImage 45, 778–787.

Koch, W., Teipel, S., Mueller, S., Buerger, K., Bokde, A., Hampel, H., Coates, U., Reiser, M., Meindl, T., in press. Effects of aging on default mode network activity in resting state fMRI: Does the method of analysis matter? NeuroImage .

Kokkonen, S.-M., Nikkinen, J., Remes, J., Kantola, J., Starck, T., Haapea, M., Tuominen, J., Tervonen, O., Kiviniemi, V., 2009. Preoperative localization of the sensorimotor area using independent component analysis of resting-state fMRI. Magnetic Resonance Imaging 27, 733–740.

Laufs, H., 2008. Endogenous brain oscillations and related networks detected by surface EEG-combined fMRI. Human Brain Mapping 29, 762–769.

Li, K., Guo, L., Nie, J., Li, G., Liu, T., 2009. Review of methods for functional brain connectivity detection using fMRI. Computerized Medical Imaging and Graphic 33, 131–139.

Margulies, D. S., Vincent, J. L., Kelly, C., Lohmann, G., Uddin, L. Q., Biswal, B. B., Villringer, A., Castellanos, F. X., Milham, M. P., Petrides, M., 2009. Precuneus shares intrinsic functional architecture in humans and monkeys. Proceedings of the National Academy of Sciences of the U.S.A. 106, 20069–20074.

Marrelec, G., Bellec, P., Benali, H., 2006. Exploring large-scale brain networks. Journal of Physiology, Paris 100, 171–181.

Mesulam, M., 2009. Defining neurocognitive networks in the BOLD new world of computed connectivity. Neuron 62, 1–3.

Nakamura, T., Hillary, F. G., Biswal, B. B., 2009. Resting network plasticity following brain injury. PLoS One 4, e8220.

Perlbarg, V., Marrelec, G., 2008. Contribution of exploratory methods to the investigation of extended large-scale brain networks in functional MRI—methodologies, results, and challenges. International Journal of Biomedical Imaging 2008, article ID 218519, 14 pages.
URL doi:10.1155/2008/218519

Raichle, M. E., Snyder, A. Z., 2007. A default mode of brain function: A brief history of an evolving idea. NeuroImage 37, 1083–1090.

Rogers, B. P., Morgan, V. L., Newtonb, A. T., Gore, J. C., 2007. Assessing functional connectivity in the human brain by fMRI. Magnetic Resonance Imaging 25, 1347–1357.

Seeley, W. W., Crawford, R. K., Zhou, J., Miller, B. L., Greicius, M. D., 2009. Neurodegenerative diseases target large-scale human brain networks. Neuron 62, 42–52.

Shimony, J. S., Zhang, D., Johnston, J. M., Fox, M. D., Roy, A., Leuthardt, E. C., 2009. Resting-state spontaneous fluctuations in brain activity: a new paradigm for presurgical planning using fMRI. Academic Radiology 16, 578–583.

Shmuel, A., Leopold, D. A., 2008. Neuronal correlates of spontaneous fluctuations in fMRI signals in monkey visual cortex: Implications for functional connectivity at rest. Human Brain Mapping 29, 751–761.

Smith, S. M., Fox, P. T., Miller, K. L., Glahn, D. C., Fox, P. M., Mackay, C. E., Filippini, N., Watkins, K. E., Toro, R., Laird, A. R., Beckmann, C. F., 2009. Correspondence of the brain's functional architecture during activation and rest. Proceedings of the National Academy of Sciences of the U.S.A. 106, 13040–13045.

Superkar, K., Menon, V., Rubin, D., Musen, M., Greicius, M. D., 2008. Network analysis of intrinsic functional brain connectivity in alzheimer's disease. PLoS Computational Biology 4, e1000100.

Superkar, K., Musen, M., Menon, V., 2009. Development of large-scale functional brain networks in children. PLoS Biology 7, e1000157.

Tomassini, V., Jbabdi, S., Klein, J. C., Behrens, T. E., Pozzilli, C., Matthews, P. M., Rushworth, M. F., Johansen-Berg, H., 2007. Diffusion-weighted imaging tractography-based parcellation of the human lateral premotor cortex identifies dorsal and ventral subregions with anatomical and functional specializations. The Journal of Neuroscience 27, 10259–10269.

van den Heuvel, M. P., Hulshoff Pol, H. E., in press. Exploring the brain network: A review on resting-state fMRI functional connectivity. European Neuropsychopharmacology .

van den Heuvel, M. P., Mandl, R. C., Kahn, R. S., Hulshoff Pol, H. E., 2009. Functionally linked resting-state networks reflect the underlying structural connectivity architecture of the human brain. Human Brain Mapping 30, 3127–3141.

Van Dijk, K. R. A., Hedden, T., Venkataraman, A., Evans, K. C., Lazar, S. W., Buckner, R. L., 2010. Intrinsic functional connectivity as a tool for human connectomics: theory, properties, and optimization. Journal of Neurophysiology 103, 297–321.

Vanhaudenhuyse, A., Noirhomme, Q., Tshibanda, L. J.-F., Bruno, M.-A., Boveroux, P., Schnakers, C., Soddu, A., Perlbarg, V., Ledoux, D., Brichant, J.-F., Moonen, G., Maquet, P., Greicius, M. D., Laureys, S., Boly, M., 2010. Default network connectivity reflects the level of consciousness in non-communicative brain-damaged patients. Brain 133, 161–171.

Vincent, J. L., Patel, G. H., Fox, M. D., Snyder, A. Z., Baker, J. T., Van Essen, D. C., Zempel, J. M., Snyder, L. H., Corbetta, M., Raichle, M. E., 2007. Intrinsic functional architecture in the anaesthetized monkey brain. Nature 447, 83–86.

Wang, J., Wang, L., Zang, Y., Yang, H., Tang, H., Gong, Q., Chen, Z., Zhu, C., He, Y., 2009. Parcellation-dependent small-world brain functional networks: a resting-state fMRI study. Human Brain Mapping 30, 1511–1523.

Wang, K., Liang, M., Wang, L., Tian, L., Zhang, X., Li, K., Jiang, T., 2007. Altered functional connectivity in early Alzheimer's disease: a resting-state fMRI study. Human Brain Mapping 28, 967–978.

Zhang, D., Johnston, J. M., Fox, M. D., Leuthardt, E. C., Grubb, R. L., Chiconoine, M. R., Smyth, M. D., Snyder, A. Z., Raichle, M. E., Shimony, J. S., 2009. Preoperataive sensorimotor mapping in brain tumor patients using spontaneous fluctuations in neuronal activity imaged with functional magnetic resonance imaging: initial experience. Neurosurgery 65, 226–236.

Zuo, X.-N., Kelly, C., Adelstein, J. S., Klein, D. F., Castellanos, F. X., Milham, M. P., 2010. Reliable intrinsic connectivity networks: Test-retest evaluation using ICA and dual regression approach. NeuroImage 49, 2163–2177.

Figure Legends

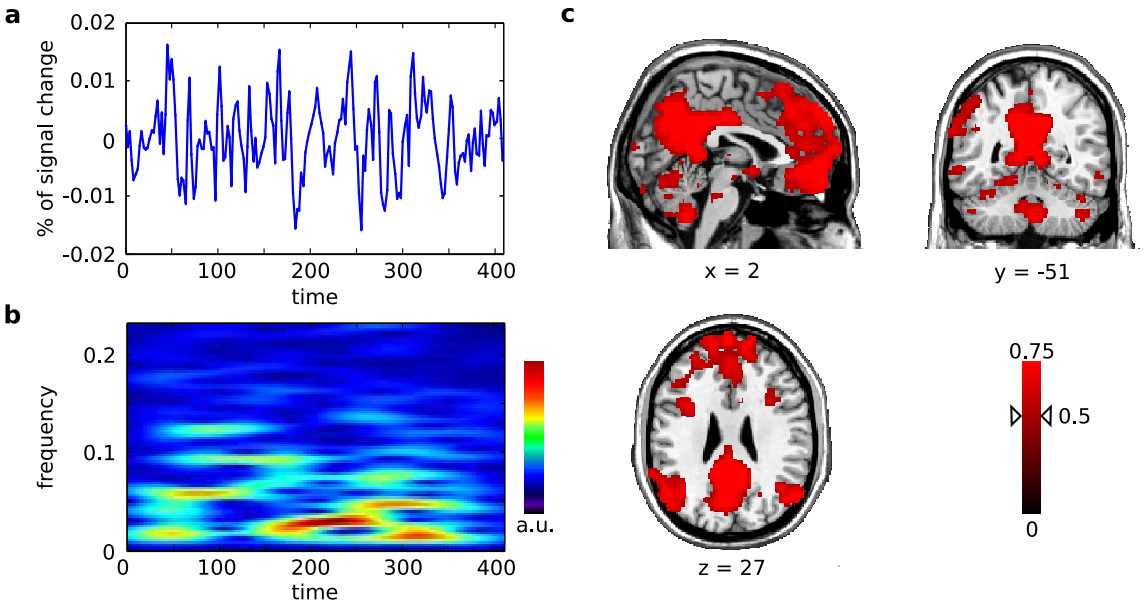

Figure 1: **Resting-state functional connectivity maps.** An individual functional connectivity map of the default-mode network was derived using the posterior cingulate seed used in Greicius et al. (2003). The time series of the seed is presented in panel **a** and is dominated by slow frequency fluctuations (below 0.1 Hz), as evidenced by a window Fourier transform representing the power spectrum as a function of time (panel **b**). A correlation map (with an arbitrary threshold of 0.5) between the time series of the seed and that of all other brain voxels identify an extended set of regions known as the default-mode network.

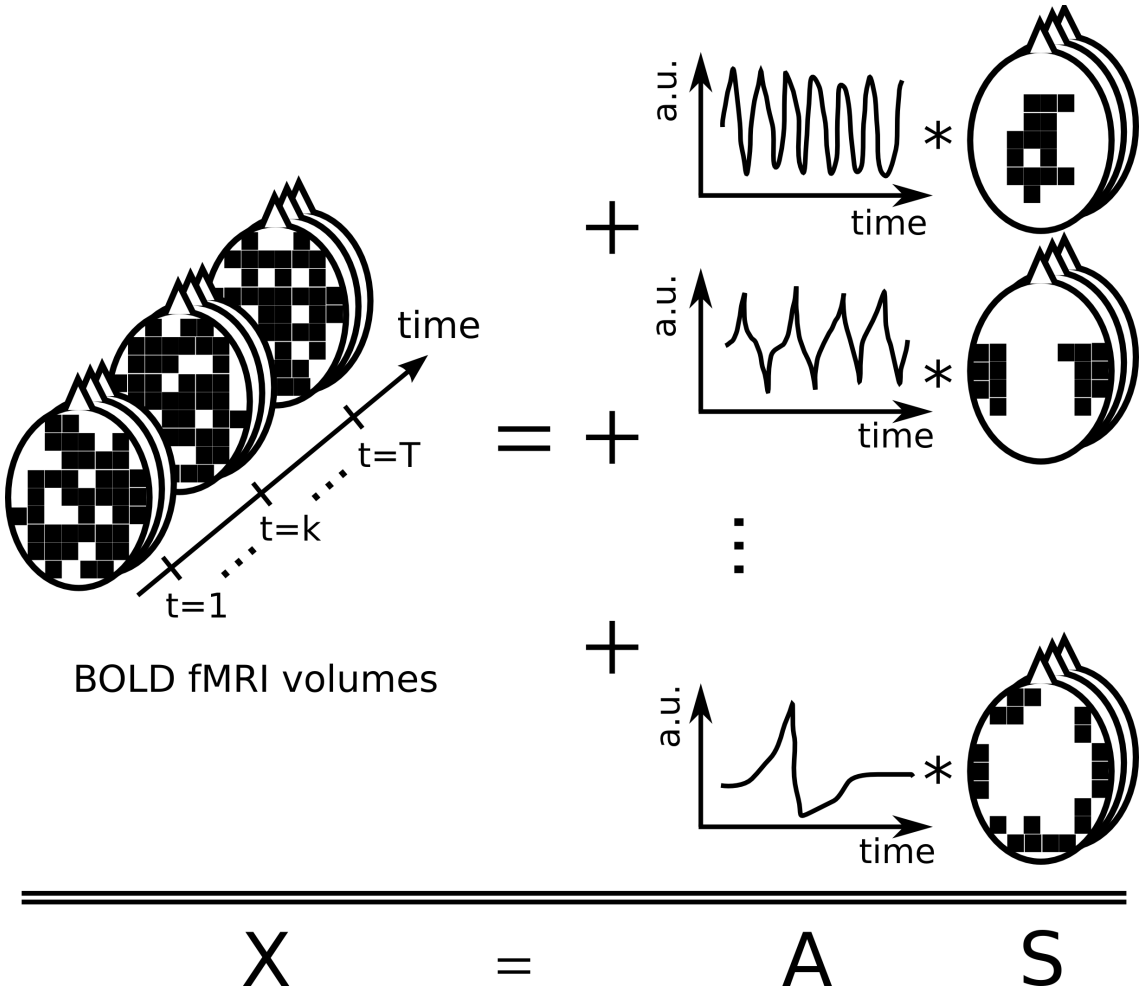

Figure 2: **Linear model for spatial independent component analysis (sICA).** ICA is based on the same linear mixture model that is used in conventional task activation paradigms. According to this model, the space-time fMRI dataset is decomposed into a number of components, each component consisting of a spatial map (in matrix S) and an associated time course (in matrix A). The spatial component describes the weight of the associated time course at each voxel. By contrast with task activation experimental designs, ICA proceeds by estimating simultaneously the spatial and temporal components. It is then possible to test for the significance of the contribution of a particular spatial component at each voxel.

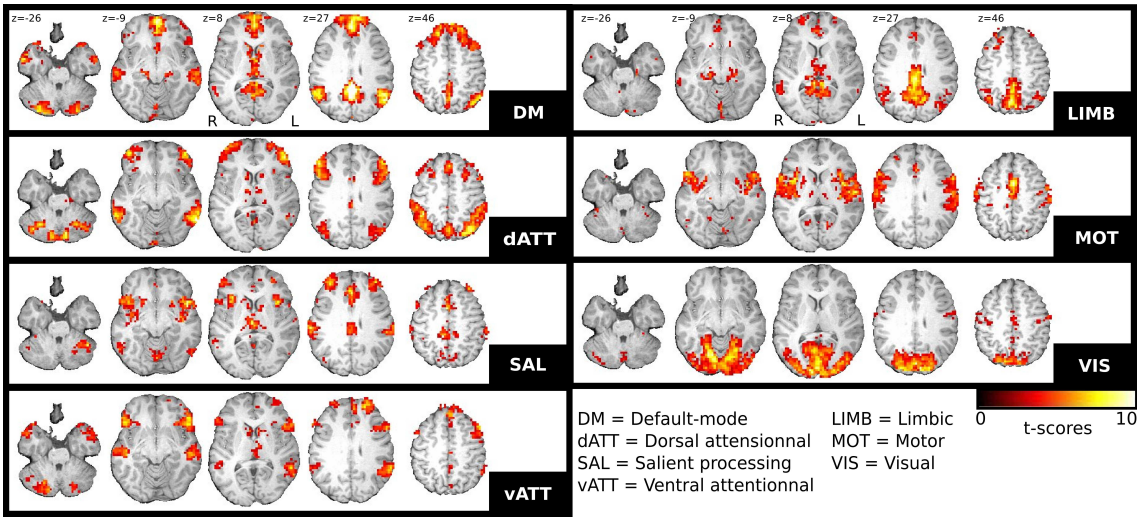

Figure 3: **Example of RSNs extracted with group ICA.** Group RSNs maps from 20 subjects scanned at rest extracted using hierarchical clustering of individual maps.

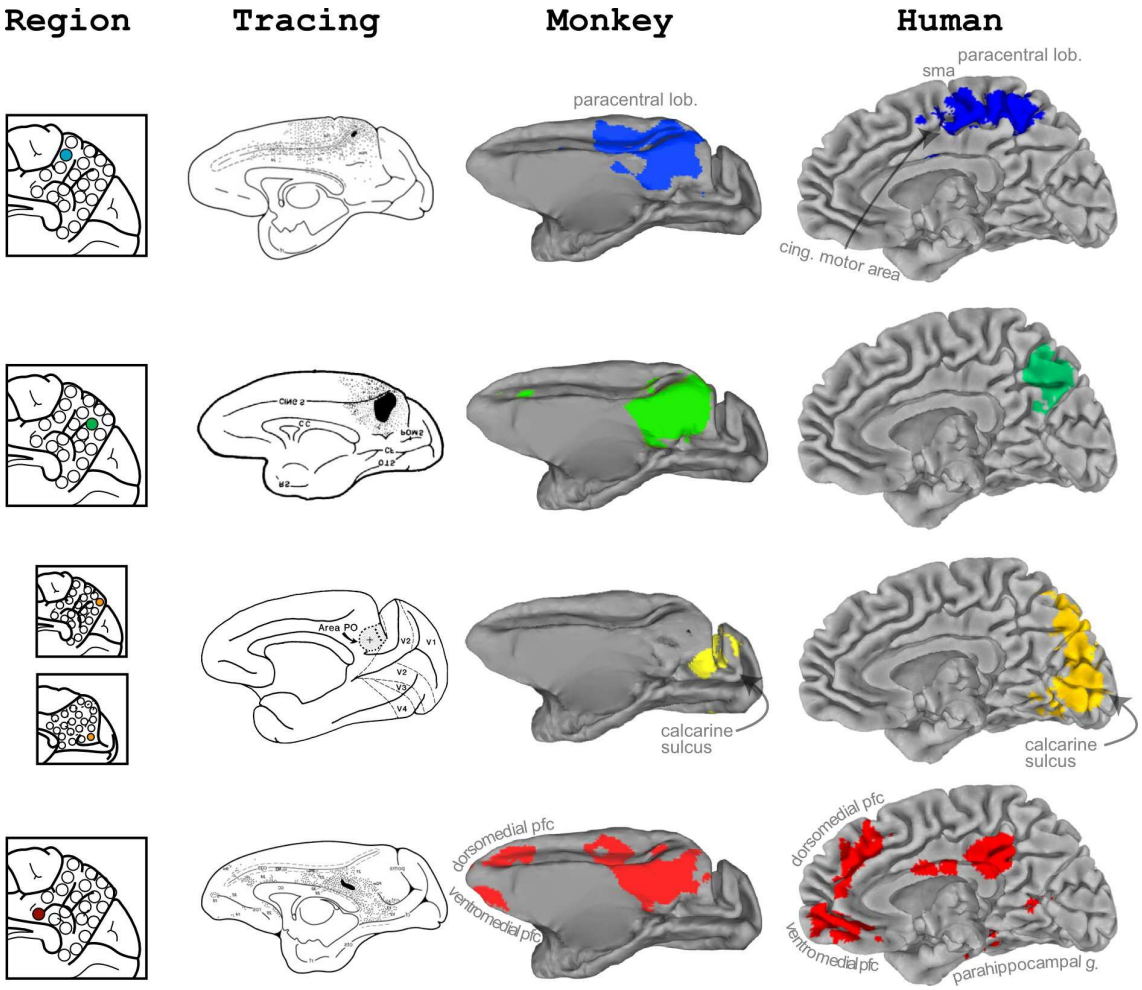

Figure 4: **Functional and anatomical parcelations of the precuneus areas in the human and monkey.** Four seed regions (left column) have been used to exemplify the markedly different patterns of functional connectivity found in the precuneus area for humans (right column) and macaque monkeys (middle right column). Similar patterns of functional connectivity were identified in both species, which were consistent with the anatomical connections of the seed regions as identified using tracers in macaques (middle left column). Figure adapted from Margulies et al. (2009), courtesy of Pr. Milham and Pr. Petrides on behalf of the co-authors.

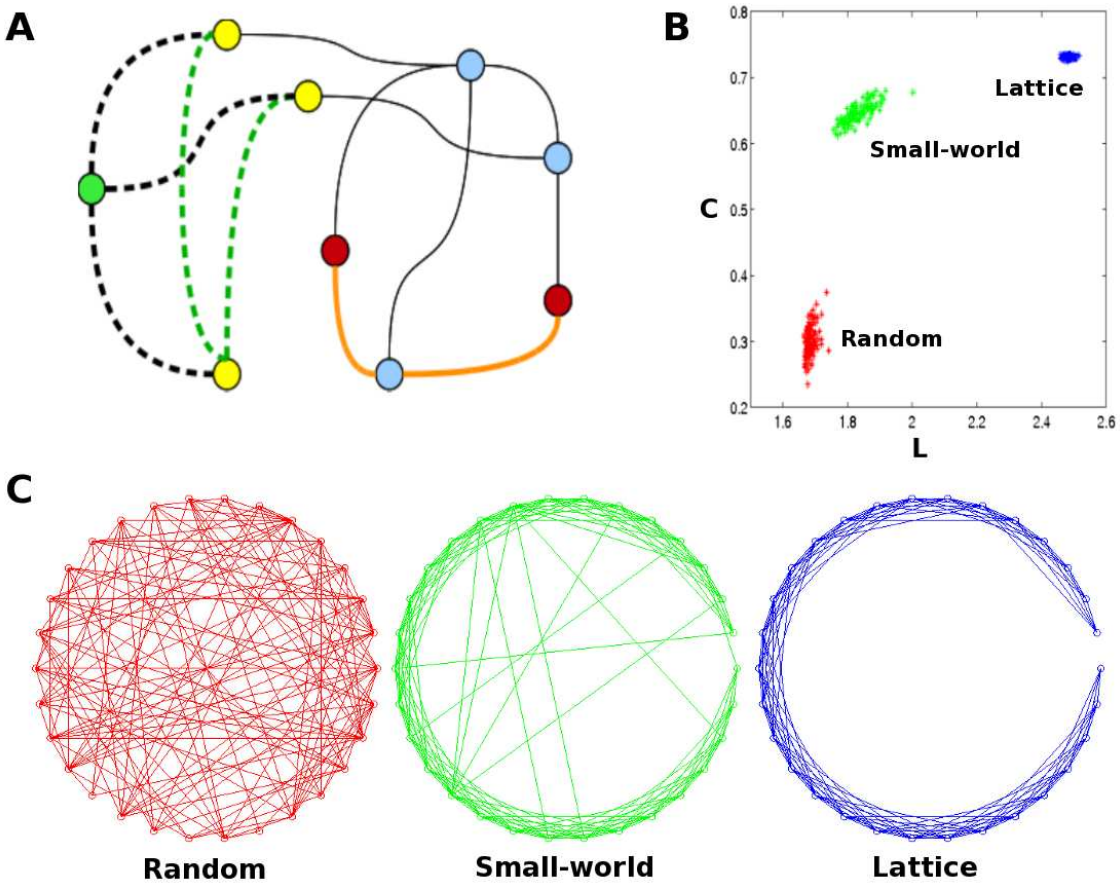

Figure 5: **Characteristic path length and clustering coefficient as key measures of graph theory.** The characteristic path length L of a network is the average length of the shortest path between any two nodes, where the path length (also called distance) between two nodes is defined as the minimum number of distinct edges required to link these nodes. The clustering coefficient C of a network C is the average of the clustering coefficients of all nodes, where the clustering coefficient of a node is the ratio between the actual number of edges among the node neighbors and the largest possible number of such connections. (A) Example of graph with 9 nodes and 12 edges. The path length between the red nodes is $L = 2$, corresponding to the shortest path (in orange) between the two nodes. The green node has 3 neighbors (in yellow), connected to it by dashed edges. These 3 nodes could potentially be connected by up to $3 \times (3-1)/2 = 3$ edges, but are effectively connected by only 2 edges (in green) in the present graph. The clustering coefficient is therefore equal to $C = 2/3$. (B) Example of characteristic path length and clustering coefficient for simulated random, small-world, and lattice graphs with the same number of nodes and edges. (C) Example of such graphs.

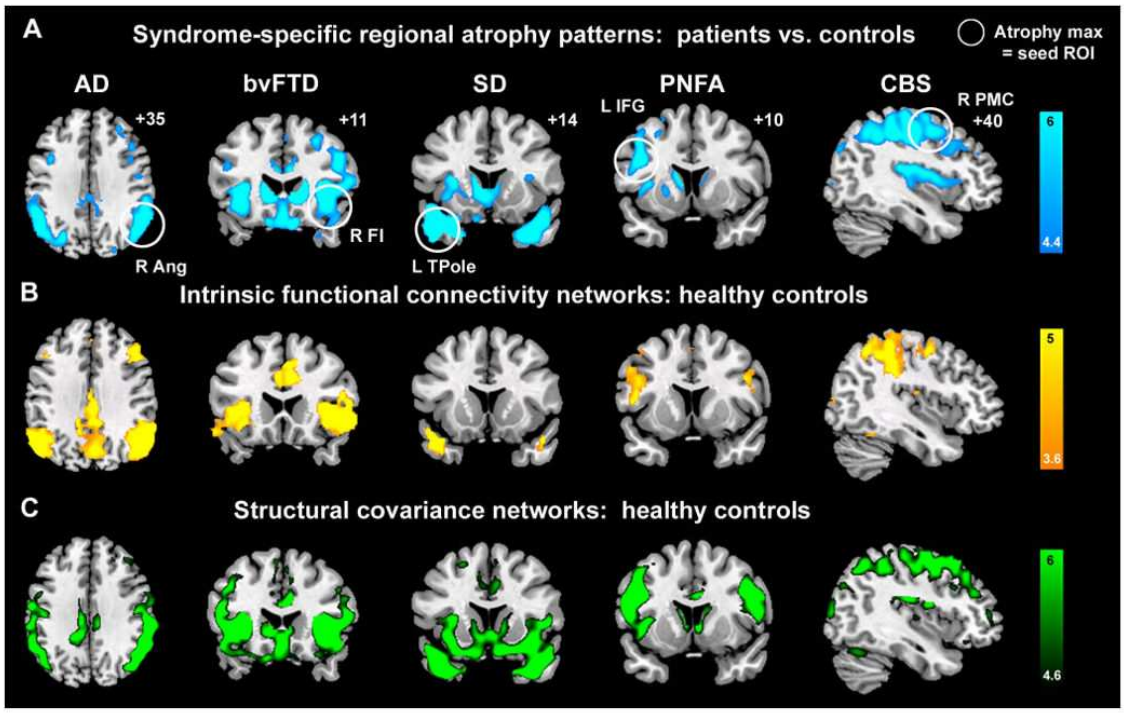

Figure 6: **Convergent syndromic atrophy, healthy RSNs, and healthy structural covariance patterns.** (from (Seeley et al., 2009)) (A) Five distinct clinical syndromes showed dissociable atrophy patterns, whose cortical maxima (circled) provided seed ROIs for RSN and structural connectivity analyses. (B) RSN mapping experiments identified five distinct networks anchored by the five syndromic atrophy seeds. (C) Healthy subjects further showed gray matter volume covariance patterns that recapitulated results shown in (A) and (B). For visualization purposes, results are shown at $p < 0.00001$ uncorrected (A and C) and $p < 0.001$ corrected height and extent thresholds (B). In (A)–(C), results are displayed on representative sections of the MNI template brain. In coronal and axial images, the left side of the image corresponds to the left side of the brain. ANG = angular gyrus; FI = frontoinsula; IFGoper = inferior frontal gyrus, pars opercularis; PMC = premotor cortex; TPole = temporal pole.